

Article

The Strengths and Limitations in Using the Daily MODIS Open Water Likelihood Algorithm for Identifying Flood Events

Catherine Ticehurst *, Juan Pablo Guerschman and Yun Chen

CSIRO Land and Water Flagship, G.P.O. Box 1666, Canberra, ACT 2601, Australia;

E-Mails: Juan.Guerschman@csiro.au (J.P.G.); Yun.Chen@csiro.au (Y.C.)

* Author to whom correspondence should be addressed; E-Mail: catherine.ticehurst@csiro.au;
Tel.: +61-2-6246-5842.

External Editors: Guy J.-P. Schumann, Richard Gloaguen and Prasad S. Thenkabail

Received: 27 June 2014; in revised form: 4 November 2014 / Accepted: 13 November 2014 /

Published: 27 November 2014

Abstract: Daily, or more frequent, maps of surface water have important applications in environmental and water resource management. In particular, surface water maps derived from remote sensing imagery play a useful role in the derivation of spatial inundation patterns over time. MODIS data provide the most realistic means to achieve this since they are daily, although they are often limited by cloud cover during flooding events, and their spatial resolutions (250–1000 m pixel) are not always suited to small river catchments. This paper tests the suitability of the MODIS sensor for identifying flood events through comparison with streamflow and rainfall measurements at a number of sites during the wet season in Northern Australia. This is done using the MODIS Open Water Likelihood (OWL) algorithm which estimates the water fraction within a pixel. On a temporal scale, cloud cover often inhibits the use of MODIS imagery at the start and lead-up to the peak of a flood event, but there are usually more cloud-free data to monitor the flood's recession. Particularly for smaller flood events, the MODIS view angle, especially when the view angle is towards the sun, has a strong influence on total estimated flood extent. Our results showed that removing pixels containing less than 6% water can eliminate most commission errors when mapping surface water. The exception to this rule was for some spectrally dark pixels occurring along the edge of the MODIS swath where the relative azimuth angle (*i.e.*, angle between the MODIS' and sun's azimuth angle) was low. Using only MODIS OWL pixels with a low view angle, or a range distance of less than 1000 km, also improves the results and minimizes multi-temporal errors in flood identification and extent. Given these limitations, MODIS

OWL surface water maps are sensitive to the dynamics of water movement when compared to streamflow data and does appear to be a suitable product for the identification and mapping of inundation extent at large regional/basin scales.

Keywords: MODIS OWL; inundation mapping; MODIS view angle

1. Introduction

Regular mapping of surface water location and extent, often at a daily or more frequent temporal scale, has important applications in environmental monitoring, water resource management, and flood emergency response. Contemporary remote sensing technologies provide an affordable means of capturing flood extent at points in time with reasonable spatial and temporal coverage. For flood monitoring there is a need for routinely acquiring remote sensing data which have regional coverage at an acceptable spatial resolution. Landsat imagery can provide the appropriate spatial detail for many water mapping applications ([1,2]), but its temporal frequency of 16 days is not suited to capturing the spatial dynamics of many flood events. Optical systems such as NASA's MODIS sensor have been used for mapping surface water at a medium spatial resolution. While the resolution of the MODIS sensor may not be ideal for mapping small water features such as narrow river channels, the spatial and temporal consistency can still be of great value in detecting general changes in water movement.

The MODIS sensors (TERRA and AQUA) can be used for mapping flood events due to their near-global spatial (250–1000 m) and temporal characteristics (1–2 times/day). Furthermore, all historical data from 2000 to present are readily available. MODIS bands 1 (Red) and 2 (NIR) are at 250 m pixel size which can be used to map flooding [3]. However, given that there is a strong sensitivity of the SWIR (Short Wave InfraRed) wavelength to water [4,5], the MODIS SWIR bands (500 m pixel size) have been utilized for inundation mapping particularly through the use of indices such as the Normalized Difference Water Index (NDWI) [6] and the modified Normalized Difference Water Index (mNDWI) [5]. The Dartmouth Flood Observatory (DFO) has developed a process to capture large global flood events [7,8], which has been further enhanced through the NASA Near Real Time (NRT) MODIS Global Flood Map [9], where daily MODIS flood maps are produced at a global scale at 250 m pixel size. The NASA/DFO algorithm uses a threshold of the SWIR band (Band 7) to help identify water pixels, as well as a ratio of the Red and NIR bands. To help reduce the effects of cloud cover, the images are composited over 2, 3 and 14-day periods [10], providing daily products of each. The 14-day NRT MODIS Global Flood Map also provides the percentage of time that a pixel is wet over this period. Water fraction mapping of MODIS pixels has also been applied at the larger pixel size. Weiss and Crabtree [11] used the Normalized Difference Vegetation Index (NDVI), NDWI and tasseled cap to derive water fraction at a 1 km pixel with reasonable accuracy but it was computationally intensive. Guerschman *et al.* [12] used a detailed empirical approach with the MODIS bands, utilizing the strong relationship between NDVI, NDWI, the SWIR bands and surface water, producing fractional water coverage at 500 m pixel size—also referred to as the Open Water Likelihood index (OWL). One of the advantages of the OWL algorithm is that it is fast and easy to apply on multi-temporal datasets, compared to more complex un-mixing algorithms.

Cloud cover is always an issue when trying to map flood events using optical remote sensing data, especially during the rising stage of a flood event. To help reduce the effects of cloud interference, the use of 8-day (MOD09A1) or 16-day (MCD43A4) MODIS composites (provided by NASA) has proven useful in mapping the temporal dynamics of water [11,13–18]. However some of the temporal detail may be lost through the compositing process [12], which makes MODIS composites inadequate for fast moving floods.

Daily MODIS OWL water maps have already been used for wetland inundation mapping [19], estimating overbank flood recharge [20], as well as assisting in the calibration of hydrodynamic models at different stages of a flood event [21], all with varying degrees of success. When compared to upstream and downstream flow measurements for the Fitzroy River and Macquarie Marshes (both in Australia) during a large flood event, the daily MODIS OWL water extent shows temporal changes as expected [22]. Ticehurst *et al.* [22] and Chen *et al.* [19] have shown that the MODIS OWL can effectively map medium to large water features when compared to an equivalent Landsat water map, but lacks the detail around the edge of a flood or along narrow water features where it tends to underestimate water extent. Even so, our experience has found the MODIS OWL to be better at identifying fine water features and open water bodies with MODIS data than the commonly used modified NDWI.

While the MODIS OWL water extent shows good correspondence to streamflow measurements for the duration and peak of medium to large floods, multi-temporal inconsistencies have been found in MODIS OWL flood extents (e.g., [20]), which are exaggerated for low streamflows. Based on this observation, this paper investigates the temporal reliability of daily MODIS OWL water maps for detecting flood events, using case studies from areas which are expected to flood and areas which are not, as well as a permanent water body. The influence of sensor view angle (including the influence of sun position) on flood extent is also examined, as well as comparisons of the MODIS OWL with other MODIS flood maps. The abilities and challenges of using the MODIS OWL to map flood extent are discussed. The paper concludes with a list of recommendations on the use of the daily MODIS OWL for mapping flood events.

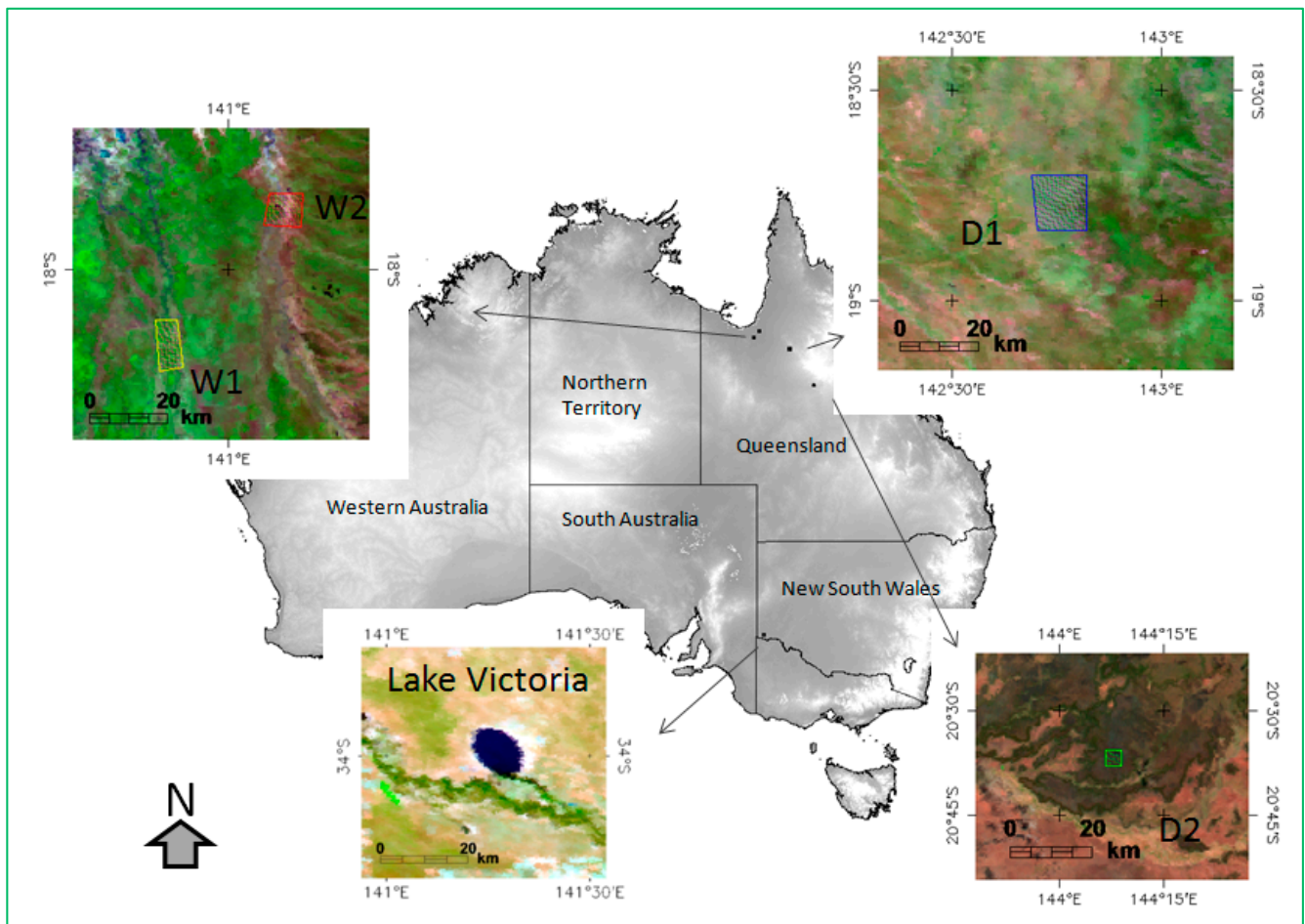
2. Study Sites

Lake Victoria is a permanent water body and of regular shape, hence it was selected for studying the stability of the MODIS OWL water extent through time (Figure 1). Lake Victoria is part of the Chowilla Riverland Floodplain straddling the South Australia (SA)—New South Wales (NSW) border. The floodplain covers a total area of 177.8 km², 74% of which lies in SA, with the remaining 26% in NSW [23]. It consists of a series of anabranch creeks, wetlands, lakes and floodplains, as well as the main Murray River channel.

Four test sites were selected to test the ability of the MODIS OWL in identifying flood events (Figure 1). These sites are located in the Gulf region of northeast Queensland in Australia. This area has a semi-arid tropical climate with 80% of its annual rainfall occurring during the wet season (November to April inclusive) [24]. Two of these sites were on a river near a streamflow gauge (sites W1 and W2), and two were in areas that are never expected to flood (sites D1 and D2)—to test for commission errors. Site D2 is located in the Gilbert catchment, while the remaining sites are in or adjacent to the Flinders catchment, which have an average annual rainfall of 775 and 492 mm respectively [24]. Nearby rainfall

data were collected for each of these sites to investigate the relationship between flood extent, streamflow (for the two sites on a river) and rainfall. For each test site, a region of interest (ROI) was selected for collecting MODIS OWL statistical data.

Figure 1. Locality map of the two dry (D1 and D2) and two wet (W1 and W2) sites, as well as Lake Victoria, Australia.



Site D1 is situated on the edge of the Gregory Ranges (Queensland, Australia) with the Gilbert River to the east, and the Yappar River to the southwest. The ROI is centered at 18.76° south, 142.75° east, covering an area of approximately 178 km^2 at an average height of $270 \text{ m AHD} \pm 20 \text{ m}$. Southwest of the site the Yappar River valley drops to heights of less than 200 m AHD . Vegetation in this area consists of mid-height open forest [25], and the soil type consists of shallow sandy/stony soils [26]. Given its location, this site is never expected to flood.

Site D2 is situated on the plateau to the north of the locality of Hughenden (Queensland, Australia). The region of interest is located on a plateau with an average height of $400 \text{ m AHD} \pm 10 \text{ m}$. There is a relatively steep drop in height of over 100 m from the plateau to the valley containing Canterbury Creek near Hughenden, which is part of the upper reaches of the Flinders River. The ROI is centered at 20.65° south, 144.12° east, with an area of 15 km^2 . The vegetation in this area is mostly grassland [25] on cracking clay soils in a basalt landscape [26]. Given its location, this site is never expected to flood.

Site W1 is located at Walkers Bend on the Flinders River (Queensland, Australia) at flow gauge station 9150003A. This lowland site is on the floodplains of the Flinders River with an average height

of 13 m AHD \pm 2 m. The ROI is centered at 18.16° south, 140.85° east with an area of 76 km². The river is flanked by riparian vegetation. The river width around this site can extend to over 100 m during the wet season, however during large floods overbank flow occurs. Daily flows of greater than 500,000 mL in volume have been recorded. Over the past 10 years, peak flow has ranged from 24,000 mL during the 2006–2007 wet season, up to 506,000 mL during the 2008–2009 wet season, with an average peak flow of 209,000 mL.

Site W2 is located at Glenmore Weir on the Norman River (Queensland, Australia) at flow gauge station 916001B. This site has an average height of 9 m AHD \pm 5 m and the ROI is centered at 17.86° south, 141.13° east covering an area of 78 km². The river is flanked by riparian vegetation. The river width can extend to around 50 m during the wet season, and overbank flow can occur for the larger floods. Streamflow records (916001B) at this site show daily streamflows of greater than 250,000 mL volume has been recorded. Over the past 10 years, peak flow has ranged from 4982 mL during the 2004–2005 wet season, up to 275,000 mL during the 2008–2009 wet season, with an average peak flow of 83,000 mL.

3. Data

TERRA and AQUA MODIS daily surface reflectance data (named MOD09GA and MYD09GA, respectively) were available from the NASA LP DAAC (Land Processes Distributed Active Archive Center) website [27]. These data are acquired daily, MOD09GA in the morning (~10:30 am local time) and MYD09GA in the afternoon (~2 pm local time), and have been atmospherically corrected [28]. For this study TERRA (MOD) and AQUA (MYD) data were downloaded from 1st November until 15th December 2002 for MODIS tile H29V12 to cover Lake Victoria at a time of year that is relatively cloud free. All data for the 2003, 2004, 2009 and 2010 wet seasons (January to April, November to December) were downloaded for MODIS tiles H31V10 and H31V11 to cover sites D1, D2, W1 and W2. These years were chosen such that it included the early and later years of the historical MODIS data, and included small and large flood events. Both 2009 and 2010 were particularly wet years in northern Australia. Only data from the wet season was analyzed because during the dry period the rivers tend to dry up completely and there is generally no recorded streamflow during the dry season. Additionally, MODIS data for tile H31V10, and the MSW (MODIS Surface Water) 2-day composite NRT shape files [10], were downloaded for January to March in 2012 to coincide with a relatively large flood event since the daily NRT Global Flood Mapping products began. This enabled a direct comparison of the two independent MODIS flood mapping methods.

Streamflow data for Walkers Bend (9150003A), and Glenmore Weir (916001B), along with rainfall data from the Australian Bureau of Meteorology for Walkers Bend and Glenmore Weir (Esmeralda Station, No. 29016), Gregory Range (Yaramulla Station, No. 30154) and Hughenden (Hughenden Station, No. 30025) were downloaded for the 2003, 2004, 2009 and 2010 wet seasons to coincide with the MODIS data for sites D1, D2, W1 and W2. Streamflow data was also acquired for January to March in 2012 to coincide with the downloaded NRT MSW product.

4. Method

MODIS OWL Water Maps

The method used for mapping open surface water was developed by Guerschmann *et al.* [12] using empirical statistical modeling and is summarized here. It calculates the fraction of water within a MODIS pixel by:

$$f_w = \frac{1}{1 + \exp(z)} \quad (1)$$

where, z is defined as:

$$z = \beta_0 + \sum_{i=0}^5 \beta_i \cdot x_i \quad (2)$$

In Equations (1) and (2), f_w is the estimated fraction of standing water, x_i are independent variables, and β_i are parameters fitted empirically. The values of β for different i are defined as follows:

$\beta_0 = -3.41375620$	
$\beta_1 = -0.000959735270$	$x_1 = \text{SWIR band 6 (reflectance*1000)}$
$\beta_2 = 0.00417955330$	$x_2 = \text{SWIR band 7 (reflectance*1000)}$
$\beta_3 = 14.1927990$	$x_3 = \text{NDVI}$
$\beta_4 = -0.430407140$	$x_4 = \text{NDWI (Gao, 1996)}$
$\beta_5 = -0.0961932990$	$x_5 = \text{MrVBF (Gallant and Dowling, 2003)}$

MrVBF is the Multi-resolution Valley Bottom Flatness index. A threshold is applied using the modified NDWI [5] where $f_w = 1$ for all mNDWI > 0.8. A cloud mask is also applied using the accompanying MODIS state band which contains information on cloud and cloud-shadow location.

For the Lake Victoria site, the TERRA (MOD) and AQUA (MYD) data were used to produce MODIS OWL water maps to allow for the effects of view angle on the MODIS OWL of a permanent water body to be examined. The number of fully inundated MODIS OWL pixels (*i.e.*, those containing 100% water in them) were counted and compared to the view angle (or range distance, *i.e.*, the distance from the sensor to the pixel) to illustrate its influence. The commonly used mNDWI [12] was also produced from the same MODIS data in order to compare MODIS OWL and mNDWI water extents for this permanent water body. The mNDWI was threshold at zero, such that pixels of zero or greater value were masked as water.

For the remaining sites (D1, D2, W1 and W2), MODIS OWL water maps from both MOD and MYD were analyzed. For each ROI, the MODIS OWL histogram containing % water values, as well as MODIS range distance (or view angle), were recorded for each daily MOD and MYD image. All ROIs containing more than 1% cloud cover were not used to ensure good data quality. A total of 206 MOD and 66 MYD scenes were used for Walkers Bend (W1), 205 MOD and 100 MYD scenes for Glenmore Weir (W2), 240 MOD and 86 MYD for Gregory Ranges (D1), and 285 MOD and 162 MYD scenes for Hughenden (D2). Daily total flood extent was recorded along with streamflow and rainfall for the same time period, to assess how well the MODIS OWL was able to detect water, and identify omission and commission errors. The reason for using coincident streamflow data was to identify the start, magnitude, duration and completion of a flood event for comparison with the daily MODIS flood extents. Rainfall data were used to assist in interpreting environmental factors that may affect the MODIS OWL pixels, such as

when there might be standing water due to large rainfall events, or when the soil might be dry due to the extended absence of rainfall. As an additional test on how well the MODIS OWL compares to other independent MODIS flood products, the MODIS OWL was compared to the NASA/DFO NRT MSW flood maps for a relatively large flood event that occurred in February 2012 at Site W1. The 2-day composite product was used to allow for a better comparison with the daily MODIS OWL data.

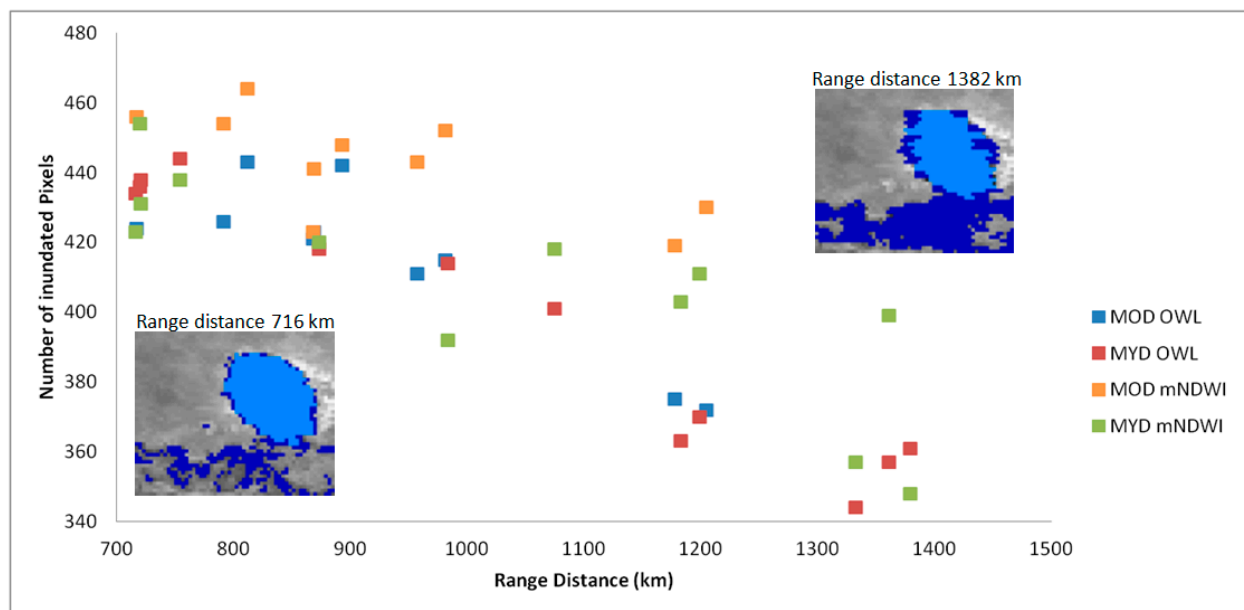
It must be emphasized that the goal of this paper is not about assessing the spatial accuracy in the distribution of flood extent. This has already been examined in [12,22,24]. The goal of this investigation is to assess the MODIS OWL's ability to detect the presence or absence of water.

5. Results

5.1. Relationship between MODIS OWL and View Angle of a Permanent Water Body

Only cloud-free MODIS scenes were used for Lake Victoria, resulting in 13 MOD scenes and 13 MYD scenes available from the start of November until mid-December 2002. When the number of inundated pixels (containing 100% water) in the MODIS OWL was regressed against sensor view angle there is an obvious linear relationship for both the MOD and MYD data (Figure 2). This relationship is also seen in the MODIS mNDWI estimate of lake extent. Lake Victoria contains around 440 wet pixels (or 110 km²) when the MODIS view angle was low (and range distance was small), which reduced to 350 wet pixels (88 km²) when the view angle was poor (and range distance was large). The influence of view angle on the number of OWL mapped inundated pixels appears to be linear with an R² of 0.77 (MOD) and 0.94 (MYD). The linear relationship is not as strong for the mNDWI mapped inundated pixels with an R² of 0.68 (MOD) and 0.47 (MYD). However the scatter is greater in the mNDWI data, particularly when only the MODIS scenes of low view angle (or range distance less than 1000 km) are used. This apparent scatter is unrelated to physical changes in water area within the lake since the reduction in the number of wet pixels is not in consecutive order, and upstream flow records indicate that streamflow is relatively low during this period. Over a period of two days the maximum change in lake size is 13 km² (or 12%) in the mNDWI data, and 7 km² (6%) in the MODIS OWL data, indicating that the MODIS OWL surface water maps are less noisy than the mNDWI for low view angles. The change in clarity and shape of the lake with respect to range distance is also obvious (Figure 2). The overall influence of view angle on a water body as large as Lake Victoria may not be substantial, but it does highlight this effect, which would be more apparent on a smaller and more irregularly shaped water body.

Figure 2. Relationship between MODIS range distance and number of inundated MOD and MYD OWL and mNDWI pixels for Lake Victoria for cloud-free images from 1st November until mid-December 2002. Two MODIS OWL images are shown as insets on the graph to further illustrate the influence of range distance (bright blue = pixels with 100% water, dark blue = less than 100% water).



5.2. Relationship between MODIS OWL, Streamflow and Rainfall Data

5.2.1. Sites not Expected to Flood (D1 and D2)

Sites D1 and D2 are areas never expected to flood, so there should be no water mapped in the MODIS OWL images. Total flood extent, as generated from the MODIS OWL, is plotted through time alongside rainfall for sites D1 (Figure 3) and D2 (Figure 4). What is most noticeable from both sites is that the MODIS OWL is mapping water during dry times, rather than wet periods (according to rainfall records). Inspection of the daily MODIS OWL histograms for Site D1 revealed most of these pixels have a % water value less than 6—that is to say there is very little water being mapped in those pixels. When all MODIS OWL pixels containing less than 6% water are removed, the total flood extent at this site is zero except for four dates (two MOD and two MYD images). The two MOD images had cloud shadow in the ROI. One of the MYD images had cloud shadow and one had a fire scar. Cloud shadow is automatically masked using the NASA generated cloud mask band, but sometimes cloud and cloud shadows are missed. Cloud shadow and fire scars appear as dark pixels which show similar spectral characteristics to water.

For Site D2, masking of pixels containing less than 6% water in the MODIS OWL data did not remove those erroneously identified as water pixels (Figure 4). Again this was occurring during dry periods. The NDVI (from the 8-day MOD13C1 product) is included in Figure 4 and it indicates that the greatest increases in MODIS OWL flood extent are occurring when the NDVI (*i.e.*, vegetation greenness) is at its lowest, so more soil is exposed to the satellite.

Figure 5 shows the total MODIS OWL water extent for pixels containing at least 6% inundation during the dry period in 2003 (MYD) and 2004 (MOD), plotted against the range distance for Site D2. These extents have been separated into those parts of the image acquired when the MODIS sensor view angle is towards the sun (*i.e.*, a small relative azimuth angle between the MODIS' and sun's azimuth angles), and away from the sun (large relative azimuth angle). The MODIS OWL values are highest for those pixels in the image where the relative azimuth angle is small, while the MODIS OWL extents are zero for those pixels where the relative azimuth angle is large. For those pixels with a small relative azimuth angle, there is a strong linear relationship with range distance. This linear relationship appears to be very similar for both the TERRA (MOD) and AQUA (MYD) MODIS sensors where the slope and intercept is (0.001, -0.58) for MOD and (0.001, -0.59) for MYD. These results suggest a 6% OWL threshold (*i.e.*, removing all OWL pixels containing less than 6% water) would remove all commission errors only for those pixels with a large relative azimuth angle.

Figure 3. Total MODIS OWL flood extent for the MOD and MYD data for Site D1, for the 2003, 2004, 2009 and 2010 wet seasons. MODIS OWL flood extent using only those pixels mapping greater than 5% inundation is also shown, along with rainfall.

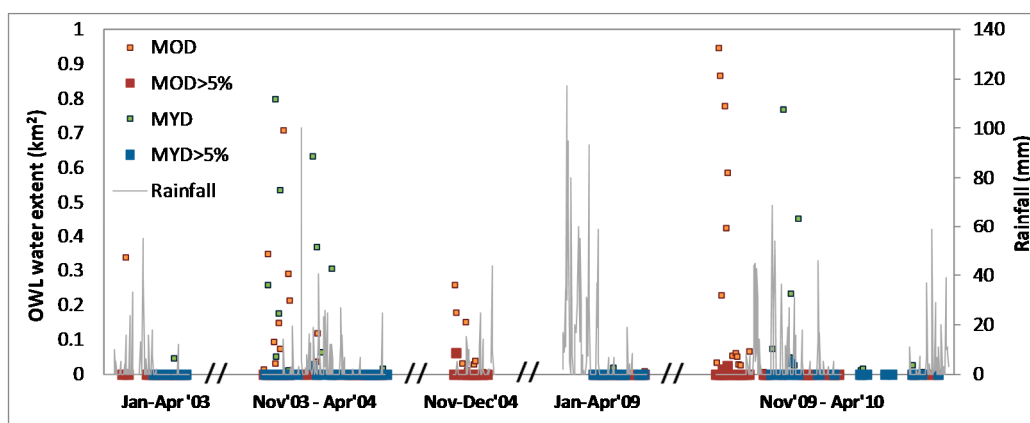


Figure 4. Total MODIS OWL flood extent for the MOD and MYD data for Site D2, for the 2003, 2004, 2009 and 2010 wet seasons. MODIS OWL flood extent using only those pixels mapping greater than 5% inundation is also shown, along with rainfall. The NDVI is also shown.

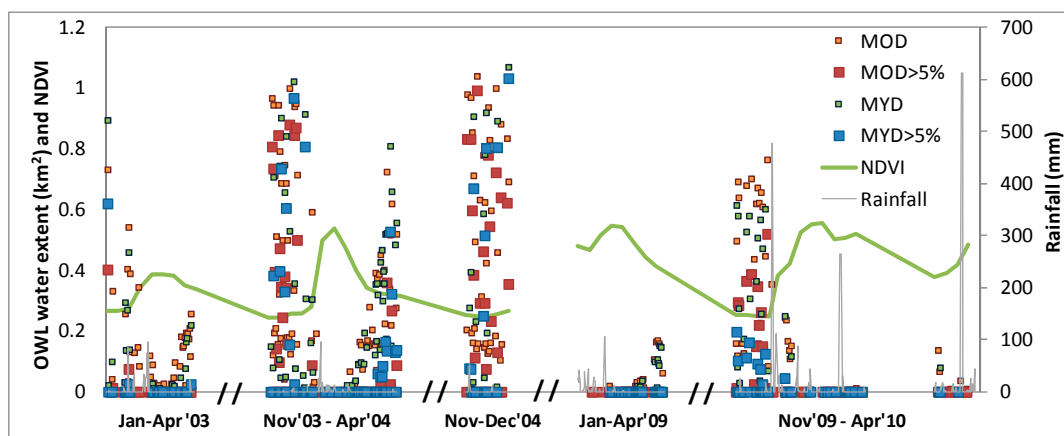
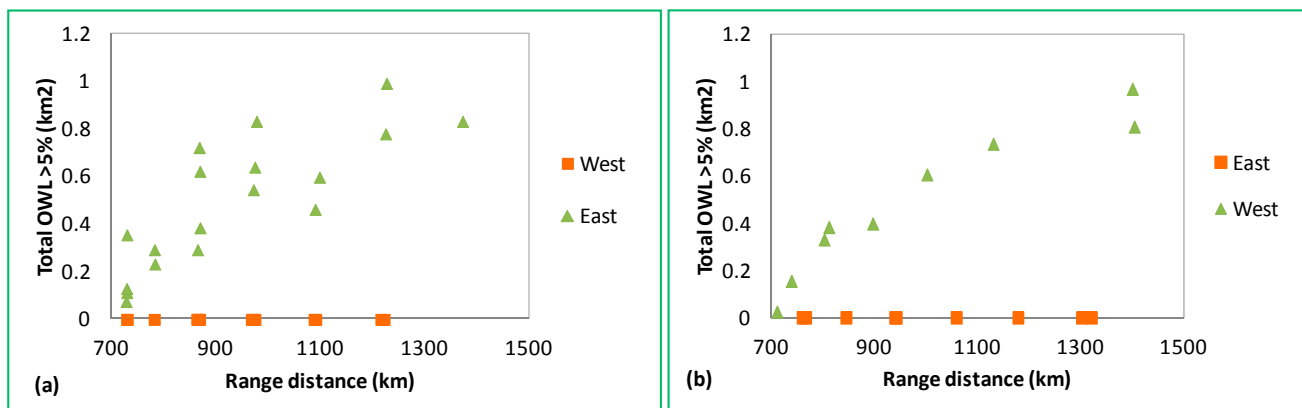


Figure 5. MODIS OWL flood extent for Site D2 for pixels mapping greater than 5% inundation plotted against range distance. The points are separated into those where the MODIS view angle is towards the sun, and those away from the sun for (a) MOD and (b) MYD data. For MOD data the direction of the sun is east, and for MYD it is west.



To test the sensitivity of the MODIS OWL threshold for eliminating commission errors, the number of pixels erroneously classified as water for sites D1 and D2 is shown in Table 1 for threshold values of 1% to 16% water. Note that those dry periods from Site D2 with a small relative azimuth angle (between the MODIS’ and sun’s azimuth angles), needed to be excluded from Table 1 for clarity (refer to Figure 4), since OWL values of up to 40% water were being erroneously identified. Previous research indicates that a MODIS OWL threshold between 3% and 6% provided best agreement when compared to an equivalent Landsat flood map [22]. Table 1 shows that apart from erroneously identifying water in four of the images (due to cloud shadow or a fire scar), a MODIS OWL threshold of 6% (*i.e.*, remove those pixels with less than 6% water) appears to work well.

Table 1. Number of pixels erroneously identified as having water for the different MODIS OWL threshold values for sites D1 and D2. All MOD and MYD data for the 2003, 2004, 2009 and 2010 wet seasons are used (with the exception of the Site D2 dry periods with a small relative azimuth angle). Those images erroneously identified as water with a 6% OWL threshold or greater contain cloud shadow (at 6% and 10%) or a fire scar (at 15%).

Data	OWL Threshold (%)															
	1	2	3	4	5	6	7	8	9	10	11	12	13	14	15	16
MOD—D1	2779	50	9	2	2	1	0	0	0	3	0	0	0	0	0	0
MYD—D1	1862	46	7	0	1	0	0	0	0	1	0	0	0	0	1	0
MOD—D2	4623	1058	380	101	18	0	0	0	0	0	0	0	0	0	0	0
MYD—D2	2235	618	368	164	52	0	0	0	0	0	0	0	0	0	0	0

5.2.2. Sites Expected to Flood (W1 and W2)

Sites W1 and W2 occur on the Flinders and Norman Rivers respectively, at streamflow gauge locations. Hence streamflow can be compared to the total MODIS OWL extent through time. Figures 6 and 7 show the MODIS OWL extent, along with streamflow and rainfall, for the 2003, 2004, 2009 and 2010 wet seasons. The MODIS OWL pixels mapping greater than 5% inundation were used to eliminate

the commission errors, as described earlier. For both the wet and dry periods, the MODIS OWL total extent matches well with the streamflow data through time. As might be expected, there is a possible lag time between the increase in streamflow and increase in the MODIS OWL water extent. This is particularly apparent for the peak of the floods in 2009 for Site W2. This is most likely due to the location of a weir within the ROI, which holds water before it spills over the top and floods downstream. It is also worth noting the limited number of MODIS OWL water maps at the start of the flood event. This is an unfortunate characteristic of optical remote sensing imagery for mapping flood events, since flooding often occurs during periods of extended cloud cover.

Figure 6. MODIS OWL flood extent (using only those pixels mapping greater than 5% inundation) for the MOD and MYD data for Site W1, for the 2003, 2004, 2009 and 2010 wet seasons. Rainfall and streamflow are also shown.

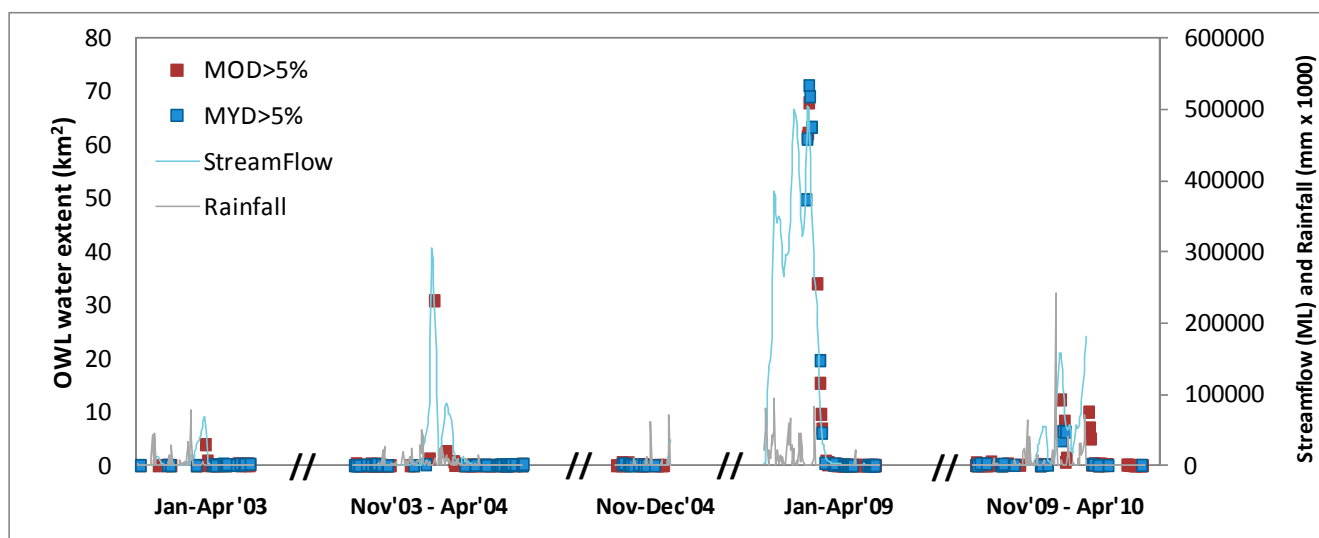
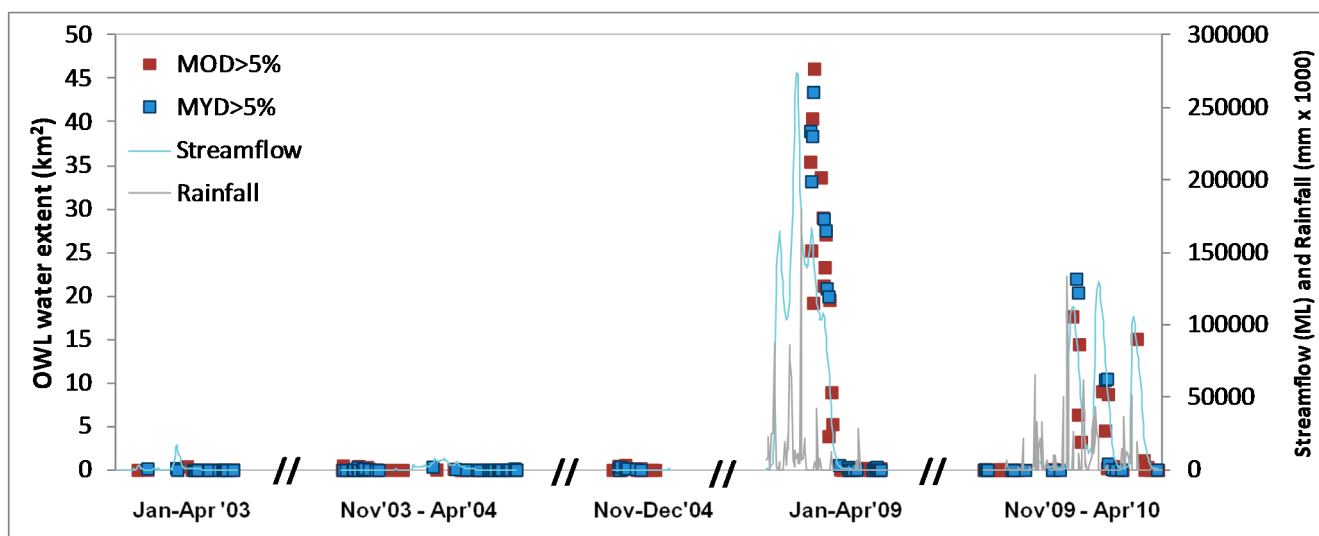


Figure 7. MODIS OWL flood extent (using only those pixels mapping greater than 5% inundation) for the MOD and MYD data for Site W2, for the 2003, 2004, 2009 and 2010 wet seasons. Rainfall and streamflow are also shown.



The MOD and MYD total flood extent is plotted against streamflow for the 2003, 2004, 2009 and 2010 wet seasons to look at the regression relationship in more detail for sites W1 and W2 (Figures 8 and 9 respectively). Those images containing a low view angle (or range distance less than 1000 km) are highlighted for both sites. The relationship between MODIS flood extent and streamflow appears to be a 2nd order polynomial, due to the delay in the increase of flood extent when compared to streamflow. The R^2 for these regression relationships are shown in the Figures. For Site W1 the relationships are very similar for the MOD and MYD flood extents compared to streamflow. Even when the large view angles (large range distance) are removed, the regression relationships do not change substantially.

The results for Site W2 have a notable improvement when the large view angles are removed (Figure 9). In general, larger view angles (large range distance) result in smaller flood extents compared to smaller view angles for both MOD and MYD data. This reduction in flood extent for the large view angle is independent of relative azimuth angle.

Figure 8. MODIS OWL flood extend plotted against streamflow for Site W1 for the 2003, 2004, 2009 and 2010 wet seasons. The data with a low view angle (lowVA), or range distance less than 1000 km, are shown in the large diamond shape.

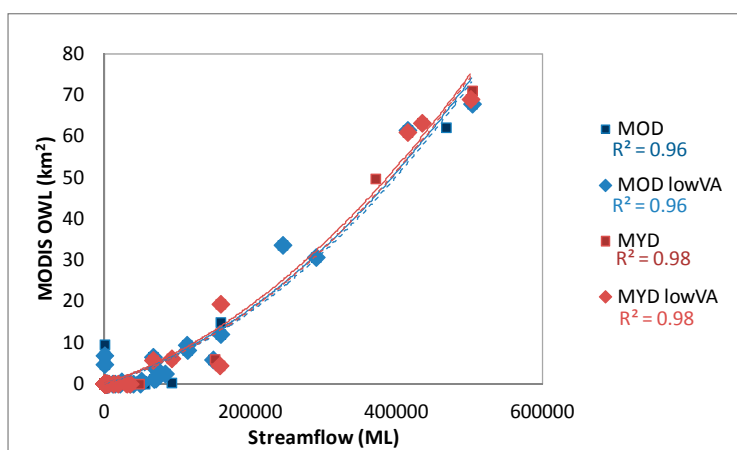
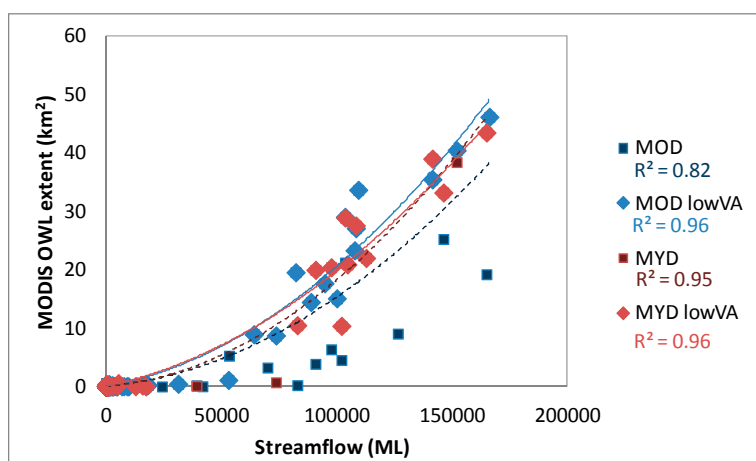
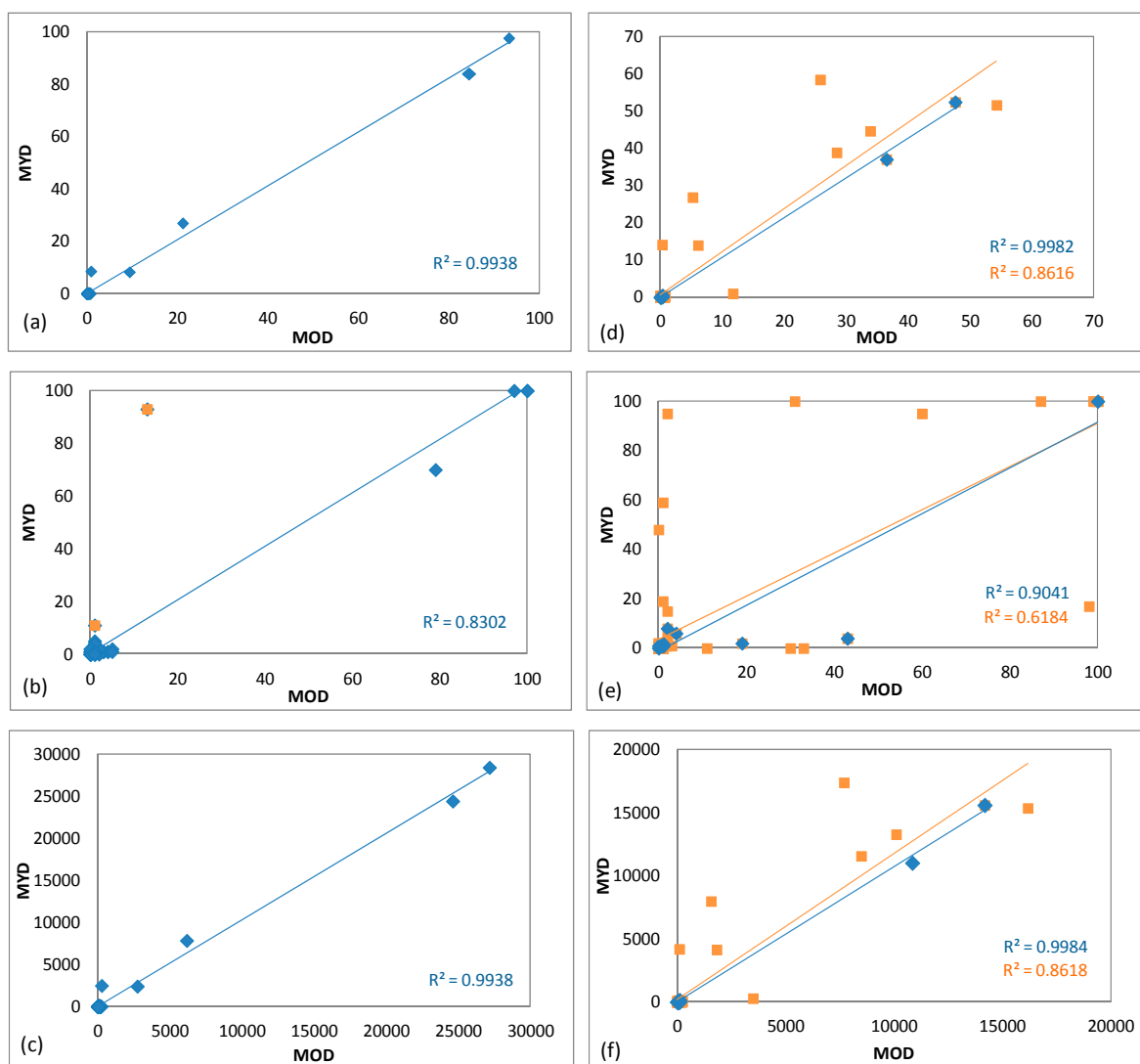


Figure 9. MODIS OWL flood extend plotted against streamflow for Site W2 for the 2003, 2004, 2009 and 2010 wet seasons. The data with a low view angle (lowVA), or range distance less than 1000 km, are shown in the large diamond shape.



The MOD and MYD OWL extents (mean, maximum and total OWL) are compared for sites W1 and W2 to determine if there is any noticeable difference between the two sensors. For Site W1 (Figure 10a–c), there is no notable difference between the MYD and MOD water maps for mean and total OWL value. For the maximum OWL value there is no difference except when there is a large difference in view angle (*i.e.*, range distance is greater than 1000 km for one of the images). In one case an outlier (shown in orange in Figure 4b) has a maximum MYD OWL value greater than 90% water when the range distance is less than 750 km, and the MOD OWL value is less than 20% water when the range distance is greater than 1250 km. A large view angle (or long range distance) will reduce the number of pixels containing high % water values (as shown in Section 5.1), and increase the number of low % water values for those pixels with a small relative azimuth angle.

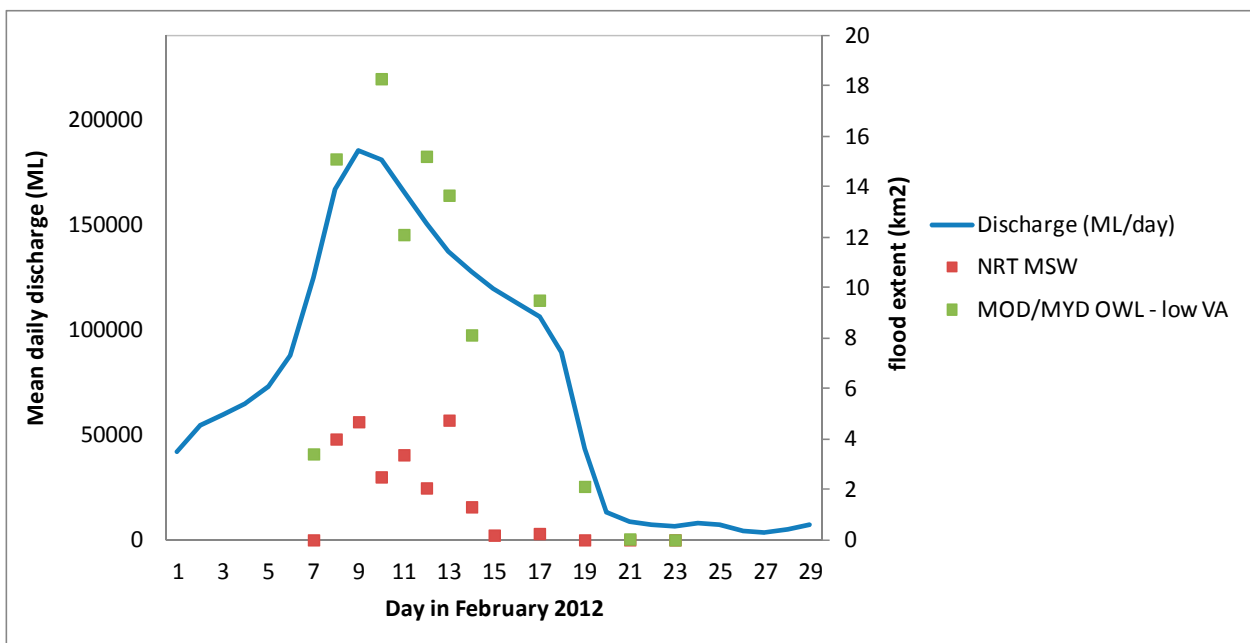
Figure 10. Mean (a), Maximum (b) and Total (c) OWL value for MYD versus MOD flood extent for the dates in common for Site W1. Mean (d), Maximum (e) and Total (f) OWL value for MYD versus MOD flood extent for the dates in common for Site W2. (Orange shows the points with a large difference in range distance between the MOD and MYD images).



For the mean and total OWL values for Site W2 there is no notable difference between the MOD and MYD flood extents for low view angles (Figure 10d–f), while there is a difference for the large view angles (*i.e.*, those with a range distance greater than 1000 km). The maximum OWL deviates from a 1:1 relationship for two of the images having a low range distance. This again can be explained by the difference in viewing angle. Even though both range distances are considered low, the MOD image has a smaller view angle (range distance 825 km) so it can see a small water feature much better than the MYD image with a larger view angle (range distance 950 km). There are large deviations from the 1:1 relationship for the maximum OWL value for those dates containing large view angles.

To test how well the MODIS OWL compares to an independent MODIS flood product, the MODIS OWL flood extent is compared to the NASA/DFO NRT flood extent of their 2-day composite product for a relatively large flood at Site W1 (Figure 11). Based on the results already shown in this paper, an OWL threshold of 6% was used and only the dates with a range distance of less than 1000 km is used. For clarity the MOD and MYD OWL flood extent are shown as the one product. Streamflow is included in Figure 11 for identifying the start, peak and end of the flood. Even though the pixel size is larger (500 m), the MODIS OWL data is identifying the flood event earlier than the NRT MSW data, as well as showing flooding for a longer period during the flood’s recession (of at least 3 days). However the MODIS OWL is mapping a much larger flood extent than the NRT MSW data. This is possibly due to the sensitivity of the SWIR band used in the MODIS OWL algorithm, but it is beyond the scope of this paper to explore further.

Figure 11. MODIS flood extent from the MODIS OWL and the NASA generated NRT MODIS Surface Water (MSW) product for Site W1 for February 2012. The MODIS OWL flood extent uses only those pixels mapping at least 6% inundation and a range distance of less than 1000 km (low View Angle) for the MOD and MYD data. Streamflow is also shown.



6. Discussion

Daily MODIS data, in this case the MODIS OWL algorithm, appears to be a suitable tool for identifying water and mapping floods, following some considerations. It is well known that indices are better for mapping water than single bands as it helps to reduce the errors associated with the solar/viewing geometry. However, indices alone still vary with the solar/viewing geometry [29] and their application is not always a simple process. Kwak *et al.* [13] used a new index with the NIR and SWIR bands, but still needed to apply some water flow rules using a DEM to reduce its errors. Hu's [29] Floating Algae Index (FAI) algorithm was designed to minimize the aerosol and solar/viewing geometry effects which can create multi-temporal spatial variation in a water-land threshold. Although it was designed for open oceans and coastal waters, Feng *et al.* [30] applies the FAI algorithm along with a within-scene spatial gradient for detecting the land-water boundary for Poyang Lake in China with encouraging results. When indices are not used, a method of temporal normalization is needed to correct for this variation in reflectance across the swath. Ward *et al.* [3] used a series of pseudo-invariant features to normalize the images. This method works well when such features are available, but may be difficult in areas of limited development.

Large view angles have always been an issue in MODIS data, e.g., [31]. Regardless of the method used to map water with the MODIS sensors, there is distortion in the pixel shape, and visibility is reduced for pixels with a large view angle. Narrow water features that are visible in pixels of low view angles can disappear altogether for large view angles.

While the MODIS OWL algorithm has some issues when identifying floods (as shown in this paper), our past experience has found the MODIS OWL to be an effective algorithm for mapping surface water for a number of reasons: it uses a standard algorithm, that can be quickly applied to all data (like the NDVI and mNDWI); it can map finer water features and has less omission errors for open water bodies compared to the often used mNDWI; and its SWIR band makes it more sensitive to water than the NDVI. Furthermore, for low view angles, the results presented here also show the MODIS OWL to be less noisy than the mNDWI for the multi-temporal monitoring of a permanent water body. This paper acknowledges the issues associated with the MODIS OWL algorithm, and attempts to quantify its effect when identifying flood events in daily MODIS OWL data. For the MODIS OWL results presented here, a 6% OWL threshold appears to remove all commission errors except for those pixels having a low relative azimuth angle. The reason why this effect is occurring is because the reflectance reduces when looking into the sun, so for the OWL algorithm (Equations (1) and (2)) the single SWIR bands are more influenced by the sun direction compared to the normalized indices (*i.e.*, NDVI and NDWI). The 6% OWL threshold can eliminate the commission errors in Site D1 but not for Site D2, which is possibly due to the different soil and vegetation cover.

The usefulness of the MODIS OWL algorithm has already been seen in a number of applications within Australia (e.g., [20,21,32]). However to make it more robust, it is desirable to apply a simple set of rules so that the MODIS OWL algorithm is a more operational and automated procedure for mapping flood events. Based on the research presented here, some considerations are required:

- For floods with MODIS pixels containing a high percentage of water within it, the MODIS OWL flood extent will reduce as view angle (or range distance) increases. Where possible,

removing the pixels having a large view angle (or range distance greater than 1000 km) seems to improve the multi-temporal consistency.

- For MODIS pixels having a low proportion of inundation (especially for values less than 6% water) the total MODIS OWL flood extent will be larger compared to those with a low view angle. In this case, removing pixels containing less than 6% water in the MODIS OWL helps reduce commission errors (*i.e.*, where pixels are incorrectly mapped as flooded).
- For the MODIS OWL algorithm, there is no notable difference between the MOD and MYD water maps. The main difference appears to be the reduced number of MYD scenes available due to increased cloud cover occurring in the afternoons in tropical regions.
- Soil and vegetation cover may have an influence on commission errors when the relative azimuth angle is low, as seen for Site D2 which had a spectral appearance of water according to the MODIS OWL algorithm. These same errors were not seen at Site D1 when the 6% MODIS OWL threshold was applied. The use of a flood likelihood mask could be used to eliminate areas not expected to flood. Such a mask could include height information from a DEM, to ensure only valleys and lowlands are able to be mapped as water, such as Martinis *et al.* [33], which would eliminate Site D2 as a potential flood zone.
- Unfortunately remnant cloud or cloud shadow, that are not removed with the NASA generated cloud mask algorithm, cannot be automatically detected and removed. However for those pixels remaining after a flood-likelihood mask and a 6% MODIS OWL threshold is applied, a multi-temporal algorithm could be used to detect uncharacteristic spikes in flood extent. This would be a relatively simple process since the location of cloud/cloud shadow varies for each MODIS image. The NASA NRT MODIS Global Flood Map product [10] also identifies most cloud shadow as water, hence they define a pixel as wet when it has been identified as water for two or more days. For priority areas, it may be possible to develop a relationship between MODIS OWL extent and streamflow based on historical data with low view angle, and preferably good solar/viewing geometry. That way, pixels containing a large range distance could be substituted with the historical OWL extent values according to flow gauge data. However this will only work for characteristic flood events that follow historical flood patterns.

7. Conclusions and Recommendations

Our past experience has found the MODIS OWL water mapping algorithm to be useful for identifying and mapping flood events. While the influence of solar/viewing geometry on MODIS data has been readily acknowledged in the literature, this paper attempts to quantify this effect on daily MODIS OWL data to make it suitable for identifying floods events in a more automated way. The daily MODIS OWL algorithm can be used for mapping medium to large flood events, although the MODIS sensor cannot reliably map narrow water features of less than one pixel width, and there is limited data at the beginning of a flood event. When data are available, our study showed the MODIS OWL water maps can be used to identify the progression of a flood event. However there are some recommendations to apply to reduce the multi-temporal noise and incorrect identification of water in the MODIS pixel:

- Select MODIS OWL values of at least 6% water as it eliminates most commission errors.

- In some cases it may be necessary to exclude pixels having a low relative azimuth angle (*i.e.*, the angle between the MODIS' and sun's azimuth angles) as this introduces commission errors in some spectrally dark pixels. However, a flood likelihood mask will also reduce the number of spectrally dark pixels which may be confused with water.
- Use daily MODIS OWL data of low view angle (range distance less than 1000 km) where possible.
- In some situations, data may be limited and all cloud-free dates are needed regardless of range distance and solar/viewing geometry. In this case, temporal averaging could be used to reduce the daily fluctuations in flood extent and to identify outliers.

The spatial and temporal consistency of the MODIS sensors means they can be of great value in detecting and monitoring the general changes in surface water movement. Given the limitations mentioned in this study, the MODIS OWL surface water maps are sensitive to the dynamics of water movement when compared to streamflow data. Application of the recommendations described here does appear to make it a suitable product for mapping inundation extent and flood progression at regional/basin scales.

Acknowledgments

Major funding for the Flinders and Gilbert Agricultural Resource Assessment was provided by the Office of Northern Australia and the Australian Government's Northern Australia Sustainable Futures program. CSIRO co-invested through its Water for a Healthy Country and Sustainable Agricultural flagships. We would like to acknowledge the Department of Natural Resources and Mines of the Queensland Government for providing streamflow data.

Author Contributions

Catherine Ticehurst performed the main multi-temporal analysis of the MODIS OWL, and wrote most of the manuscript. Juan Pablo Guerschman developed the MODIS OWL algorithm and provided comments throughout. Yun Chen contributed to Lake Victoria description and data.

Conflicts of Interest

The authors declare no conflict of interest.

References

1. Ryu, J.-H.; Won, J.-S.; Min, K.D. Waterline extraction from Landsat TM data in a tidal flat. A case study in Gomso Bay, Korea. *Remote Sens. Environ.* **2002**, *83*, 442–456.
2. Frazier, P.S.; Page, K.J. Water body detection and delineation with Landsat TM data. *Photogramm. Eng. Remote Sens.* **2000**, *66*, 1461–1467.
3. Ward, D.P.; Hamilton, S.K.; Jardine, T.D.; Pettit, N.E.; Tews, E.K.; Olley, J.M.; Bunn, S.E. Assessing the seasonal dynamics of inundation, turbidity, and aquatic vegetation in the Australian wet-dry tropics using optical remote sensing. *Ecohydrology* **2013**, *6*, 312–323.

4. Gao, B.C. NDWI—A normalized difference water index for remote sensing of vegetation liquid water from space. *Remote Sens. Environ.* **1996**, *58*, 257–266.
5. Xu, H. Modification of normalised difference water index (NDWI) to enhance open water features in remotely sensed imagery. *Int. J. Remote Sens.* **2006**, *27*, 3025–3033.
6. McFeeters, S.K. The use of normalized difference water index (NDWI) in the delineation of open water features. *Int. J. Remote Sens.* **1996**, *17*, 1425–1432.
7. Dartmouth Flood Observatory. Available online: <http://floodobservatory.colorado.edu> (accessed on 19 November 2014).
8. Brakenridge, R.; Anderson, E. MODIS-based flood detection, mapping and measurement: The potential for operational hydrological applications. In *Transboundary Floods: Reducing Risks through Flood Management*; Marsalek, J., Stancalie, G., Balint, G., Eds.; Springer Netherlands: Berlin, Germany, 2006; pp. 1–12.
9. De Groeve, T.; Vernaccini, L.; Brakenridge, G.R.; Adler, R.; Ricko, M.; Wu, H.; Thielen, J.; Salamon, P.; Policelli, F.S.; Slayback, D.; *et al.* *Global Integrated Flood Map. A JRC Technical Report, 2012*; Publications Office of the European Union: Luxembourg, European Union, 2013.
10. NASA. NRT Global Flood Mapping. Available online: oas.gsfc.nasa.gov (accessed on 31 October 2014).
11. Weiss, D.J.; Crabtree, R.L. Percent surface water estimation for MODIS BRDF 16-day image composites. *Remote Sens. Environ.* **2011**, *115*, 2035–2046.
12. Guerschman, J.P.; Warren, G.; Byrne, G.; Lymburner, L.; Mueller, N.; Van-Dijk, A. *MODIS-Based Standing Water Detection for Flood and Large Reservoir Mapping: Algorithm Development and Applications for the Australian Continent*; CSIRO: Canberra, Australia, 2011.
13. Kwak, Y.; Park, J.; Fukami, K. Estimating floodwater from MODIS time series and SRTM DEM data. *Artif. Life Robot.* **2014**, *19*, 95–102.
14. Ordoyne, C.; Friedl, M.A. Using MODIS data to characterize seasonal inundation patterns in the Florida Everglades. *Remote Sens. Environ.* **2008**, *112*, 4107–4119.
15. Chen, Y.; Cuddy, S.M.; Wang, B.; Merrin, L.E.; Pollock, D.; Sims, N. Linking inundation timing and extent to ecological response models using the Murray-Darling Basin Floodplain Inundation Model (MDB-FIM). In *Proceedings of MODSIM2011: The 19th International Congress on Modelling and Simulation*, Perth, Australia, 12–16 December 2011.
16. Huang, C.; Chen, Y.; Wu, J. Mapping spatio-temporal flood inundation dynamics at large river basin scale using time-series flow data and MODIS imagery. *Int. J. Appl. Earth Obs. Geoinf.* **2014**, *26*, 350–362.
17. Huang, C.; Chen, Y.; Wu, J.; Yu, J. Detecting floodplain inundation frequency using MODIS time-series imagery. In *Proceedings of Agro-Geoinformatics2012: The 1st International Conference on Agro-Geoinformatics*, Shanghai, China, 2–4 August 2012.
18. Huang, S.; Li, J.; Xu, M. Water surface variations monitoring and flood hazard analysis in Dongting Lake area using long-term Terra/MODIS data time series. *Natural Hazards* **2012**, *62*, 93–100.
19. Chen, Y.; Huang, C.; Ticehurst, C.; Merrin, L.; Thew, P. An evaluation of MODIS daily and 8-day composite products for floodplain and wetland inundation mapping. *Wetlands* **2013**, *33*, 823–835.
20. Doble, R.; Crosbie, R.; Peeters, L.; Joehnk, K.; Ticehurst, C. Modelling overbank flood recharge at a continental scale. *Hydrol. Earth Syst. Sci.* **2014**, *18*, 1273–1288.

21. Karim, F.; Petheram, C.; Marvanek, S.; Ticehurst, C.; Wallace, J.; Gouweleeuw, B. The use of hydrodynamic modelling and remote sensing to estimate floodplain inundation and flood discharge in a large tropical catchment. In Proceedings of MODSIM2011: The 19th International Congress on Modelling and Simulation, Perth, Australia, 12–16 December 2011.
22. Ticehurst, C.J.; Chen, Y.; Karim, F.; Dutta, D.; Gouweleeuw, B. Using MODIS for mapping flood events for use in hydrological and hydrodynamic models: Experiences so far. In Proceedings of MODSIM2013, 20th International Congress on Modelling and Simulation, Adelaide, Australia, 1–6 December 2013.
23. MDBA (Murray-Darling Basin Authority). Chowilla Floodplain. Environmental Water Management Plan. Available online: www.mdba.gov.au/sites/default/files/pubs/CFSL_FA_screen.pdf (accessed on 27 February 2012).
24. Dutta, D.; Karim, F.; Ticehurst, C.; Marvanek, S.; Petheram, C. *Floodplain Inundation Mapping and Modelling in the Flinders and Gilbert Catchments. A Technical Report to the Australian Government from the CSIRO Flinders and Gilbert Agricultural Resource Assessment, Part of the North Queensland Irrigated Agriculture Strategy*; CSIRO Water for a Healthy Country and Sustainable Agriculture Flagships: Canberra, Australia, 2013.
25. Royal Geographical Society of Queensland. Queensland by Degrees. Available online: www.rgsq.org.au/qldbydeg (accessed on 30 April 2014).
26. Bartley, R.; Thomas, M.F.; Clifford, D.; Phillip, S.; Brough, D.; Harms, D.; Willis, R.; Gregory, L.; Glover, M.; Moodie, K.; et al. *Land Suitability: Technical Methods. A Technical Report to the Australian Government for the Flinders and Gilbert Agricultural Resource Assessment (FGARA) Project*; CSIRO: Canberra, Australia, 2013.
27. NASA. Reverb|Echo—The Next Generation Earth Science Discovery Tool. Available online: reverb.echo.nasa.gov/reverb (accessed on 19 November 2014).
28. Vermote, E.; Kitchenova, S. MOD09 (Surface Reflectance) User's Guide. Available online: modis-sr.ltdri.org (accessed on 1 May 2014).
29. Hu, C. A novel ocean color index to detect floating algae in the global oceans. *Remote Sens. Environ.* **2009**, *113*, 2118–2129.
30. Feng, L.; Hu, C.; Chen, X.; Cai, X.; Tian, L.; Gan, W. Assessment of inundation changes of Poyang Lake using MODIS observations between 2000 and 2010. *Remote Sens. Environ.* **2012**, *121*, 80–92.
31. Xin, Q.; Woodcock, C.E.; Liu, J.; Tan, B.; Melloh, R.A.; Davis, R.E. View angle effects on MODIS slow mapping in forests. *Remote Sens. Environ.* **2012**, *118*, 50–59.
32. Chen, Y.; Wang, B.; Pollino, C.A.; Cuddy, S.M.; Merrin, L.E.; Huang, C. Estimate of flood inundation and retention on wetlands using remote sensing and GIS. *Ecohydrology* **2014**, *7*, 1412–1420.
33. Martinis, S.; Twele, A.; Strobl, C.; Kersten, J.; Stein, E. A multi-scale flood monitoring system based on fully automatic MODIS and TerraSAR-X processing chains. *Remote Sens.* **2013**, *5*, 5598–5619.